Aortic Root Motion Correction in C-Arm Flat-Detector CT

Julia Wicklein, Günter Lauritsch, Kerstin Müller, Holger Kunze, Willi A. Kalender, and Yiannis Kyriakou

***Abstract*—Treatment of cardiac diseases via minimally invasive procedures is of major interest in the clinics. An angiographic C-arm CT system is state-of-the-art in an interventional cardiac laboratory. It opens up the possibility of 3D reconstruction during the procedure. Due to the long acquisition time of several seconds of the C-arm, imaging of dynamic structures is a challenging problem. Therefore, motion correction for cardiac applications is an issue for this imaging device. New minimally invasive procedures like the recently introduced TAVI (transcatheter aortic valve implantation) suffer from cardiac motion. The 3D image of the aorta is acquired during rapid pacing of the patient to minimize the cardiac motion and to reduce the blood flow. We present a new algorithmic approach for motion compensation of the aortic root for TAVI procedures under sinus rythm to make rapid pacing unnecessary. Our optimization routine was tested on three clinical datasets of the aortic root, wherein all three show promising results.**

***Index Terms*—Flat-Detector CT, Cardiac imaging, Aortic root, Motion correction.**

I. Introduction

Transcatheter aortic valve implantation (TAVI) is a minimally invasive procedure that spares high risk or elderly patients open-heart surgeries to treat severe aortic valve stenosis (see Ref. [1]). By default preoperative surgical planning is performed using 3D computed tomography (CT) images. For example the diameter of the annulus of the aortic outflow tract is measured to make the right choice for the prosthetic valve size. Modern hybrid operating rooms are equipped with fixed C-arm systems, providing the physicians with real time 2D fluoroscopic images for guidance during the surgery. Recently, the authors of Ref. [2] introduced an automatic aorta segmentation approach for TAVI.

Ref. [3] introduces a TAVI imaging procedure which makes use of the C-arm CT for both, the 3D volume and the 2D fluoroscopic images. This allows for an accurate and straightforward 2D/3D overlay during the intervention. The short interval between the 3D aquisition and the valve deployment leeds to a better reflection of the patient's anatomy during the intervention. The 3D image is aquired during a 5 seconds scan taking 248 projections over 200°. Selective contrasting was proposed. A pigtail catheter is placed in one of the cusps (typically the non-coronary cusp). Thus, only the aortic root is contrasted. Unfortunately we do not see the aortic outflow tract since this object is beyond the aortic valves. In order to minimize artifacts caused by cardiac motion, rapid ventricular pacing is applied of 180 - 220 bpm and patient breathing is supended. Figure 1 shows an aortic root segmentation illustrating the basic anatomy of a normal aortic valve with three cusps and the ostium of the two coronary arteries.

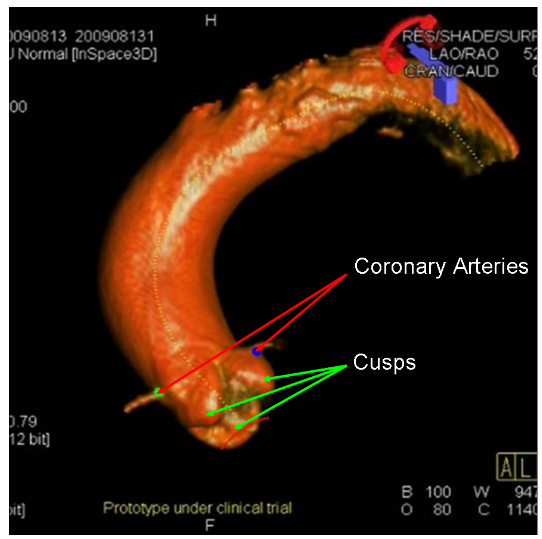

Fig. 1. 3D C-arm CT reconstruction of the aortic root with the TAVI product software from Siemens AG showing typical anatomic landmarks.

Rapid pacing might cause instabilities to the circuit of the patient. There is a clinical desire avoiding rapid pacing and performing imaging in the Sinus rhythm of the patient. Cardiac motion can be treated algorithmically by estimation of the motion from the imaging data and compensating the motion in the reconstruction step. Ref. [4] performs motion estimation on segmented projection images. The accuracy of segmentation is sensitive to the quality and the contrast to noise ratio of the images. Ref. [5] estimates the motion by 3D-3D registration of ECG-gated volume images. A long acquisition time of many heart cycles is needed in Flat Detector CT (FD-CT) for generating ECG-gated volume images (see Ref. [6]). In this paper, we present a novel algorithmic approach to reduce motion artifacts of the aortic root without the need for rapid pacing. It makes use of an entropy based motion and misalignment correction method introduced in Ref. [7].

Julia Wicklein and Willi A. Kalender are with the Institute of Medical Physics (IMP), University of Erlangen–Nürnberg, Henkestraße 91, 91052 Erlangen. Günter Lauritsch, Holger Kunze and Yiannis Kyriakou are with Siemens AG, Healthcare Sector, Forchheim, Germany. Kerstin Müller is with the Pattern Recognition Lab, Department of Computer Science and the Erlangen Graduate School in Advanced Optical Technologies (SAOT), University of Erlangen–Nürnberg, Erlangen, Germany. Corresponding author: Julia Wicklein, E-mail: julia.wicklein@imp.uni-erlangen.de.

The method was originally developed to reduce misalignment and motion artifacts for neuroradiology applications. We adopt the main part of the original approach that is responsible for motion correction tasks. In a two step procedure, aortic root motion is estimated by counteracting variations of the system geometry parameters, which are illustrated in Figure 2.

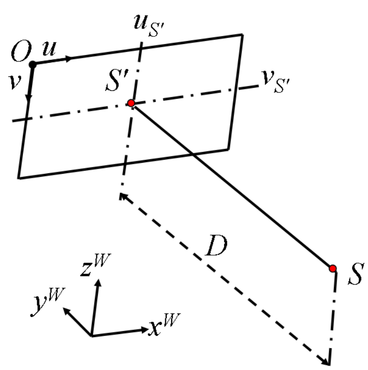

Fig. 2. FD-CT geometry according to Ref. [8]. O defines the detector origin point, S the source position, D the source-detector distance, u, v the detector coordinates and S' the projection of S onto the detector-plane. The rotation axis is parallel to the z^W-coordinate.

The efficiency of our approach was evaluated on three clinical datasets. The data was acquired with the TAVI protocol without rapid pacing. We present the results and illustrate the amenities of our motion correction method for interventional aortic root imaging in the interventional suite.

II. Method

A. Motion Artifacts Metric

In Ref. [8] several image features were investigated with respect to their sensitivity for misalignment artifacts. An entropy criterion based on the gray-level histogram of the reconstructed images was identified to be the most promising one for medical FD-CT applications. Fig. 2 shows the defined FD-CT geometry. Therefore, we chose this feature as motion artifacts metric (MAM) for our motion compensation approach. The histogram (H) of the intensity values q provides a global description of an image. Entropy E using the gray level histogram H is calculated according to:

$$E = -\sum_{q=0}^{Q} (h(q) \cdot log\ h(q)),$$

with

$$h(q) = \frac{H(q)}{N},$$

where Q is the maximum intensity value, h is the normalized histogram or probability distribution of the image and N is the number of image pixels.

B. Optimization Routine

We assume that the motion of the aorta is rigid without major deformations. Therefore, an adaption of the algorithm introduced in Ref. [7] is used to correct for cardiac motion (i.e. orgen- or respiratory motion) without a-priori information. Figure 3 illustrates the estimated parameters which are explained in the following paragraph.

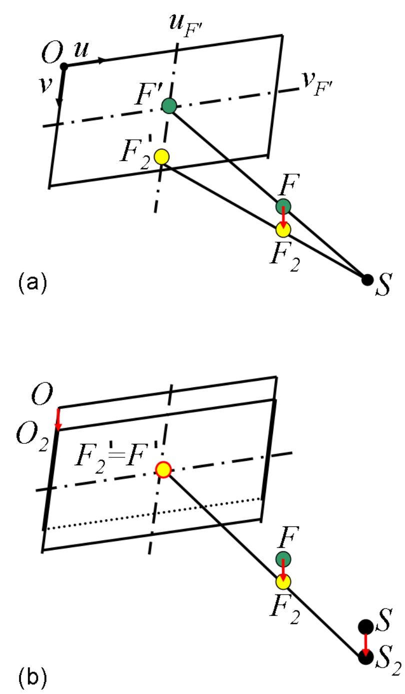

Fig. 3. Example for an object motion: The object point F moves to F_2 (translation in detector-u direction). This causes a translation of the projection of F onto the detector-plane from F' to F_2' (a). Compensation with simultanious detector and source translation (from O to O_2 and from S to S_2) (b).

The movement of the object is compensated by an appropriate variation of the underlying system geometry. A number of four system parameters need to be estimated for motion correction. Parameters like detector- or source-translation or a detector rotation are used to compensate patient motion. Figure 3(a) shows an object translation in detector-u direction. Figure 3(b) shows the compensation by translating detector and source in the same direction. Furthermore a translation in detector v-direction and a detector rotation is optimized to correct object motion in 3D-space.

During the optimization routine, the MAM criterion is used to estimate the mentioned parameters. This is done by minimizing the entropy of the reconstructed images within a gradient descent algorithm with adaptive step size, based on Newton's method:

$$x^{k+1} := x^k + \alpha^k d^k,$$

with

$$d^k = f''(x^k)^{-1}(-f'(x^k)),$$

for updating the function value x^k from iteration k to $k+1$, where d^k defines the Newton-direction with a constant α. The secant method is used to approximate the two derivatives $f'(x^k)$ and $f''(x^k)$ of the optimization function f, representing the MAM criterion:

$$f'(x^k) \approx \frac{f(x^k+1) - f(x^k-1)}{(x^k+1) - (x^k-1)},$$

$$f''(x^k) \approx \frac{f(x^k+1) + f(x^k-1) - 2f(x^k)}{(\frac{(x^k+1)-(x^k-1)}{2})^2}.$$

Entropy minimization is performed during a blockwise and a projectionwise parameter optimization. We reconstructed three transverse slices (z = 0, z = 20 pixels, z = -20 pixels) for the optimization algorithm with a size of 256 pixels $\times$ 256 pixels and a pixel size of 0.5 mm $\times$ 0.5 mm.

1) Blockwise Optimization: The first step iteratively adjusts blocks of projections covering a certain range of the scan. This range enables the correction for cardiac without conflicts of different heart phases. These are adjusted through a number of iterations.

2) Projectionwise Optimization: The second step performs projectionswise adjustments of the whole scan within a few iterations. This procedure removes streak artifacts caused by deviations of single projections.

III. Measurements

We evaluated three datasets scanned with 248 projections over 200° using the Siemens Artis zeego system (Siemens AG, Healthcare Sector, Forchheim, Germany) with a detector of size 616 pixels $\times$ 480 pixels and a pixel size of 0.616 mm $\times$ 0.616 mm, a source-isocenter distance of 785 mm and a source-detector distance of 1200 mm. The aortic root was contrasted with a pigtail catheter placed close to the aortic valve.

IV. Results

The proposed algorithm for motion compensation of the aortic root was evaluated on three clinical datasets. Figures 4, 5 and 6 show the preliminary results. The original standard FDK reconstruction according to Ref. [9] is displayed in (a). It is visible that the image quality of the FDK reconstruction is degraded by motion artifacts. The three leaflets are highly corrupted by motion blur. The motion corrected reconstructions in Figure 5(b), 6(b) and 7(b) show the improvements in the area of the aortic root. Each Subfigure shows the multi-planar reconstruction images (long axis view top left and right, short axis view bottom left) and volume rendering (bottom right).

The results presented in Figure 4, 5 and 6 demonstrate the effect of the optimization approach. The aortic roots after optimization appear less artifact afflicted. The cusps of the aortic valve and even the commissures of the leaflets are specifiable after applying the correction routine. We tested the approach on three different datasets, wherein all three show comparable good results.

V. Conclusions

The first results with the new motion correction algorithm on three clinical datasets show very promising results. The motion correction approach works without a-priori knowledge and gives the possibility to do interventional aortic root imaging without the need for rapid pacing or with less contrast agent insertion.

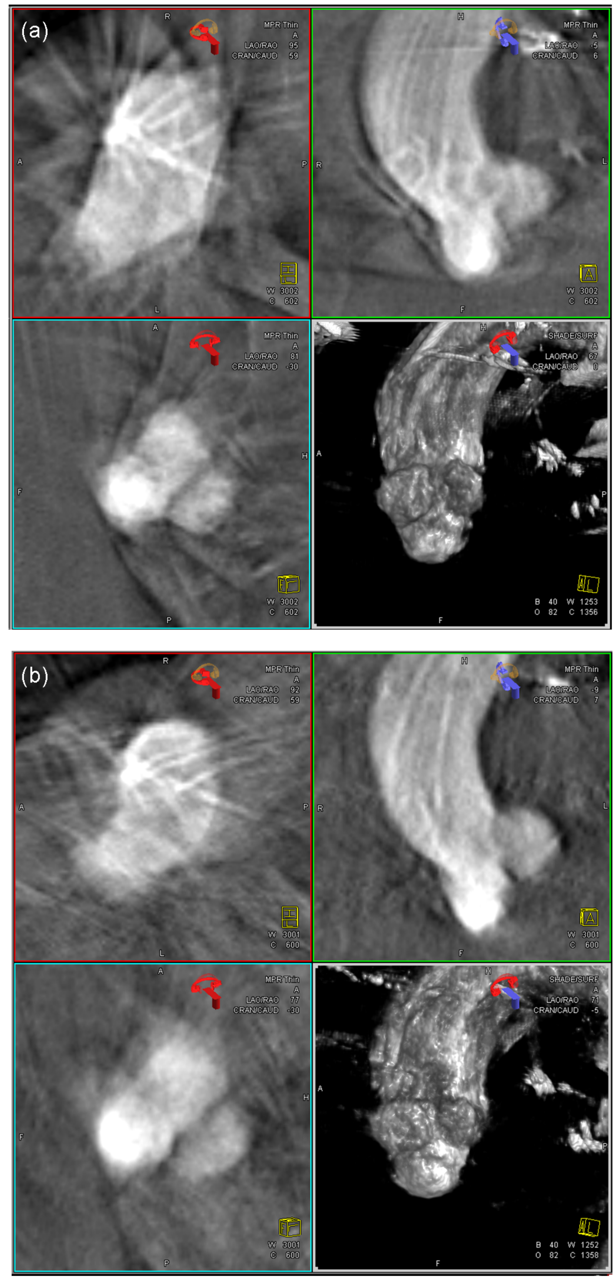

Fig. 4. Aortic root reconstruction of dataset 1: Original (a). Optimization result (b). Each including the saggital cut ($x = 0$, upper left), the coronal cut ($y = 0$, upper right), the transverse cut ($z = 0$, lower left) and the volume image (lower right).

VI. Acknowledgement

The authors would like to thank Prof. James N. Slater of the NYU Langone Medical Center for providing clinical datasets.

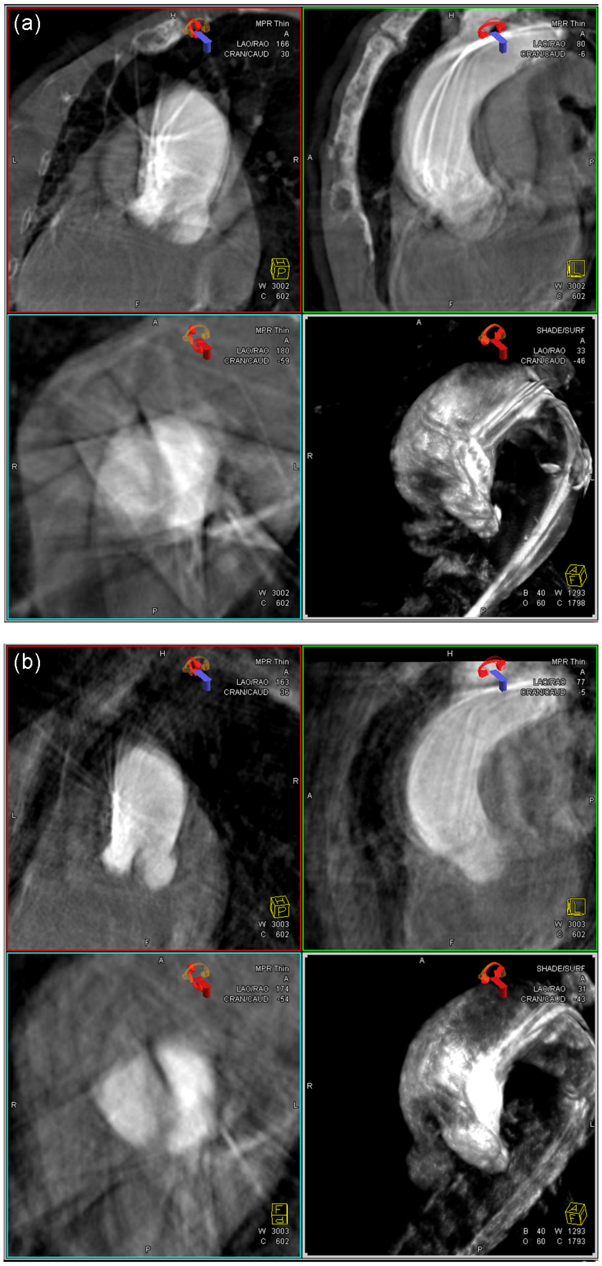

Fig. 5. Aortic root reconstruction of dataset 2: Original (a). Optimization result (b). Each including the saggital cut ($x = 0$, upper left), the coronal cut ($y = 0$, upper right), the transverse cut ($z = 0$, lower left) and the volume image (lower right).

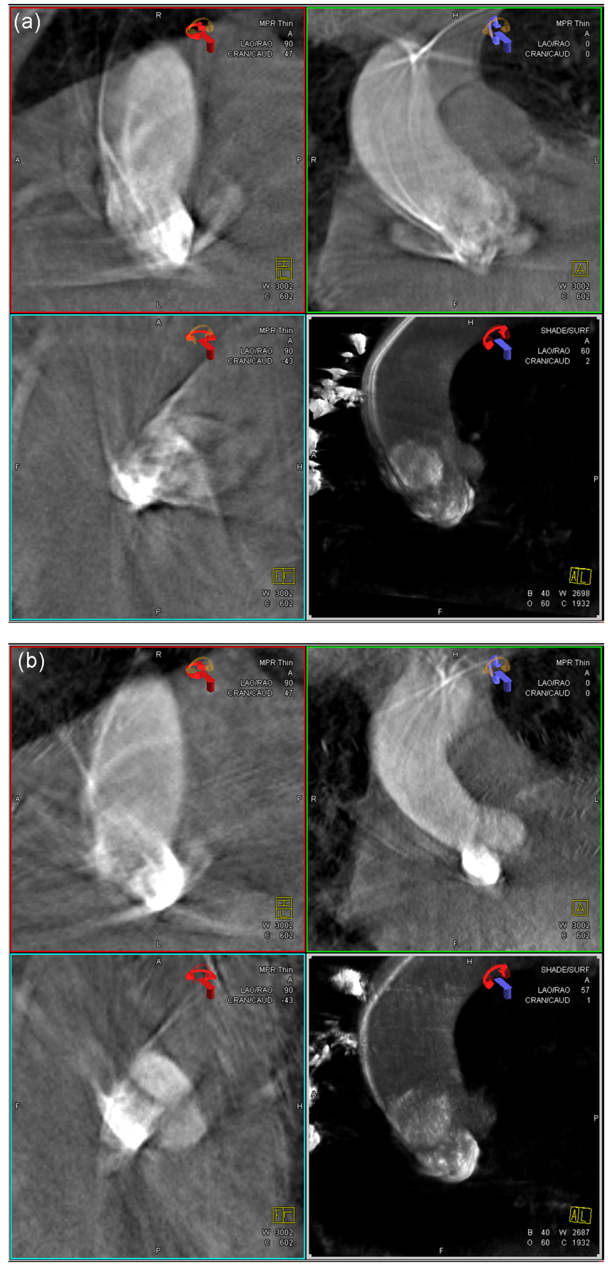

Fig. 6. Aortic root reconstruction of dataset 3: Original (a). Optimization result (b). Each including the saggital cut ($x = 0$, upper left), the coronal cut ($y = 0$, upper right), the transverse cut ($z = 0$, lower left) and the volume image (lower right).

The concepts and information presented in this paper are based on research and are not commercially available.

REFERENCES

[1] M. B. Leon, et. al., *Transcatheter Aortic-Valve Implantation for Aortic Stenosis in Patients Who Cannot Indergo Surgery*, N Engl J Med 2010, No. 363, pp. 1597-1607, 2010.

[2] Y. Zheng, et. al., *Automatic Aorta Segmentation and Valve Landmark Detection in C-Arm CT for Transcatheter Aortic Valve Implantation*, IEEE Transactions on Medical Imaging, Vol. 31, No. 12, pp. 2307-2321, 2012.

[3] M. John, et. al., *System to Guide Transcatheter Aortic Valve Implantations Based on Interventional C-Arm CT Imaging*, Proc. of MICCAI 2010, Part I, LNCS 6361, pp. 375-382, 2010.

[4] K. Müller, et. al., Med. Phys. 2013, to be published.

[5] K. Müller, et. al., *4-D Motion Field Estimation by Combined Multiple Heart Phase Registration (CMHPR) for Cardiac C-arm Data*, Proc. of IEEE NSS-MIC, pp. 3707-3712, 2012.

[6] S. de Buck, et. al., *A new approach for prospective gated cardiac rotational angiography*Proc. of SPIE Medical Imaging, paper 8668-104, 2013.

[7] J. Wicklein, et. al., *An online motion- and misalignment-correction method for medical flat-detector CT*, Proc. of SPIE Medical Imaging, paper 8668-62, 2013.

[8] J. Wicklein, et. al., *Image features for misalignment correction in medical flat-detector CT*, Medical Physics, Vol. 39(8), pp. 4918-4931, 2012.

[9] L. A. Feldkamp, et. al., *Practical Cone-Beam Algorithm*, JOSA A, Vol. 1, Issue 6, pp. 612-619, 1984.